



[Antioxidants \(Basel\)](#). 2021 May 5;10(5):725. doi: 10.3390/antiox10050725.

Systematic Development and Characterization of Novel, High Drug-Loaded, Photostable, Curcumin Solid Lipid Nanoparticle Hydrogel for Wound Healing

Simarjot Kaur Sandhu ¹, Suneel Kumar ², Jayant Raut ¹, Mandeep Singh ¹, Sandeep Kaur ¹, Garima Sharma ¹, Tomas L Roldan ^{3 4}, Sonia Trehan ⁵, Jennifer Holloway ^{3 4}, Gabriella Wahler ^{4 6}, Jeffrey D Laskin ^{4 6}, Patrick J Sinko ^{3 4}, Francois Berthiaume ², Bozena Michniak-Kohn ^{3 5}, Praveen Rishi ⁷, Narayanan Ganesh ⁸, Indu Pal Kaur ¹

Affiliations

PMID: 34063003 PMCID: [PMC8148018](#) DOI: [10.3390/antiox10050725](#)

[Free PMC article](#)

Abstract

The study aims to develop high drug-loaded (about 15% lipid matrix) curcumin solid lipid nanoparticles (CSLNs) for wound healing. CSLNs prepared by hot, high-pressure homogenization, without using organic solvents, were optimized using the Taguchi design followed by the central composite design. The optimized CSLNs exhibited a high assay/drug content (0.6% w/w), solubility (6×10^5 times), and EE (75%) with a particle size < 200 nm (PDI-0.143). The CSLNs were safe (in vitro and in vivo), photostable, autoclavable, stable up to one year at 30 °C and under refrigeration and exhibited a controlled release (zero-order; 5 days). XRD, FTIR, and DSC confirmed solubilization and entrapment of the curcumin within the SLNs. TEM and FESEM revealed a smooth and spherical shape. The CSLNs showed a significant antimicrobial effect (MIC of 64 $\mu\text{g}/\text{mL}$ for planktonic cells; 512 $\mu\text{g}/\text{mL}$ for biofilm formation; and 2 mg/mL for mature biofilm) against *Staphylococcus aureus* 9144, while free curcumin dispersion did not exhibit any effect. This is the first report on the disruption of mature biofilms by curcumin solid lipid nanoparticles (CSLNs). The cell proliferation potential of CSLNs was also evaluated in vitro while the wound healing potential of CSLNs (incorporated in a hydrogel) was assessed in vivo. In (i) nitrogen mustard gas and (ii) a full-thickness excision wound model, CSLNs exhibited (a) significantly faster wound closure, (b) histologically and immunohistochemically better healing, (c) lower oxidative stress (LPO) and (d) inflammation (TNF α), and (e) increased angiogenesis (VEGF) and antioxidant enzymes, i.e., catalase and GSH levels. CSLNs thus offer a promising modern wound therapy especially for infected wounds, considering their effects in mature biofilm disruption.

Keywords: TNF α ; VEGF; biofilm; nanocarriers; oxidative stress; safety; wound closure.

Figures

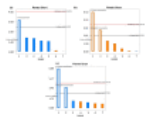


Figure 1 Pareto charts for response variable...

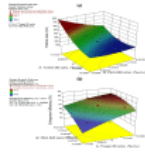


Figure 2 Response surface curves for (...)

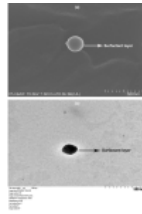


Figure 3 (a) FESEM image...

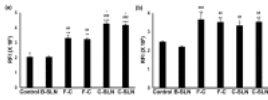


Figure 4 (a) Proliferative effect...

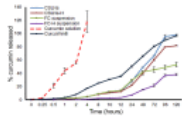


Figure 5 Cumulative % curcumin release from...

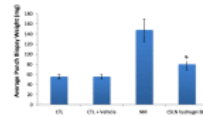


Figure 6 Average punch biopsy weight for...

All figures (11)

LinkOut - more resources

Full Text Sources

[Europe PubMed Central](#)

[Multidisciplinary Digital Publishing Institute \(MDPI\)](#)

[PubMed Central](#)

Preparation and Characterization of in-Situ Gelling Systems Containing Curcumin Loaded Solid Lipid Nanoparticles for Periodontitis

Pariksha Oberoi¹, Joga Singh¹, Garima Sharma¹, Vishakha Grover² and Indu Pal Kaur^{1*}

¹University Institute of Pharmaceutical Sciences, Chandigarh, India

²Dr. Harvansh Singh Judge Institute of Dental Sciences and Hospital, Panjab University, Chandigarh

Submission: September 17, 2021; Published: September 29, 2021

*Corresponding author: Indu Pal Kaur, UIPS, Panjab University, University Institute of Pharmaceutical Sciences, Panjab University, Chandigarh, India

Abstract

Local delivery of curcumin (Cmn) in the form of site-specific periodontal formulations can open up newer option for the management of periodontal diseases. Efficacy of such delivery systems is dependent on the sustained release of Cmn from the device in a soluble form and its penetration into the base of the periodontal pocket and adjacent connective tissue. However, Cmn finds limited clinical applications in oral environment due to its poor aqueous solubility, poor permeability, high metabolism, and instability (hydrolytic, enzymatic and photodegradation). Nanotechnology could address these shortfalls of Cmn by allowing its delivery in a solubilized, bioavailable and photostable formulation amenable for periodontal application. Encapsulation of Cmn within solid lipid nanoparticles; SLNs (C-SLNs) in our previous work has shown an increase in its water dispersibility, chemical stability and bioactivity. In the current study, we have prepared in-situ gelling system incorporating C-SLNs using poloxamer 407 as in-situ gelling agent and Carbopol 934 as mucoadhesive agent. The in-situ gelling systems showed a prolonged and sustained release up to 8 days (192h). We also tested antioxidant potential of C-SLNs and compared it with ascorbic acid and raw Cmn using DPPH in-vitro antioxidant assay kinetics. C-SLNs showed higher IC50 with respect to free Cmn solution and also ascorbic acid. At the end of 5 days, IC50 of C-SLNS was 152.12 ± 0.20 mM which was lesser than that of ascorbic acid and Cmn. Kinetic analysis of ascorbic acid, Cmn and C-SLNS also established the superior antioxidant potential of C-SLNS in comparison to ascorbic acid and Cmn. Thus, the present investigation reports the development of a sustained release Cmn loaded solid lipid nanoparticles containing formulation with good antioxidant potential which can be employed as an effective treatment option for periodontitis.

Keywords: Antioxidant potential; Nanoparticles; Kinetics assay; Dental products

Abbreviations: Cmn: Curcumin; COX-2: Cyclooxygenase-2; C-SLNs: Cmn loaded Solid Lipid Nanoparticles; DSC: Differential Scanning Calorimeter; FTIR: Fourier Transform Infra-Red; HPH: High-Pressure Homogenization; HPMC E 5: Hydroxypropyl Methylcellulose E5; I.C 50 : Half-Maximal Inhibitory Concentration; IL: Interleukin; LPS: Lipopolysaccharide; MAPKs: Mitogen-Activated Protein Kinases; NF- κ B: Nuclear Factor-Kb; PDI: Polydispersity Index; ROS: Reactive Oxygen Species; TDC: Total Drug Content; TNF- α : Tumor Necrosis Factor-Alpha; TPA : Texture Profile Analysis

Introduction

Periodontitis is a complex chronic immune inflammatory disease stimulated by long-term presence of subgingival periodontopathic biofilm (dental plaque) and is an underlying cause for loss of teeth at an early age. Severe periodontal diseases are estimated to affect nearly 10% of the global population. The red bacterial complex i.e. *P. gingivalis*; *T. denticola*; and *T. forsythia* is responsible for progression of periodontitis. The bacterial lipopolysaccharide (LPS; endotoxin) stimulates immune responses elevating cytokines and other proinflammatory mediators viz. prostaglandins; matrix metalloproteinase (MMP); subsequently causing destruction and loss of periodontal connective tissues including bone [1]. Various research studies have shown that inflammation and oxidative stress are the crucial components in the initiation and progression of periodontitis. Conventional

non-surgical/mechanical treatment with adjunct antibiotics (like *doxycycline*) therapy is reasonably successful [2]. However, antimicrobial resistance; cost and poor patient compliance due to side effects limit the use of antibiotics on a large scale. Cmn; a natural yellow phenolic compound has been extensively researched and successfully applied for the management of many chronic inflammatory diseases. It modulates the inflammatory response by down regulating the activity of cyclooxygenase-2 (COX-2) & lipoxygenase; inhibits the production of inflammatory cytokines e.g.; tumor necrosis factor-alpha (TNF- α); interleukin (IL) -1; -2; -6; -8; and -12; monocyte chemo attractant protein (MCP); and migration inhibitory protein; and modulates the activity of signaling pathways and transcription factors; especially nuclear factor- κ B (NF- κ B); activating protein- 1 (AP-1) and mitogen-activated protein kinases (MAPKs) [3-5]. It downregulates

reactive oxygen species (ROS) and malondialdehyde but does the reverse on glutathione thus showing antioxidant property. Thus, it can find use in periodontitis due to its ability to inhibit *P. gingivalis*; *Prevotella intermedia*; *Fusobacterium nucleatum*; and *Treponema denticola* [6]. Researchers have documented its inherent potential in suppression of *P. gingivalis* homotypic and *P. gingivalis*; *S. gordonii* heterotypic biofilm formation mediated mainly through inhibition of bacterial quorum sensing systems [7]. Cmn is well known inhibitor of bacterial LPS induced cytokine expression. Further it is a promotor for collagen production and fibroblastic cell numbers [8]. However, Cmn finds limited clinical in oral environment applications due to its poor aqueous solubility; permeability; high metabolism; and instability in the physiological system as well as on storage. Nanotechnology could address these shortfalls of Cmn by allowing its delivery in a solubilized; bioavailable and photostable formulation. Encapsulation within SLNs developed previously in our lab has addressed the above-mentioned pit falls associated with Cmn [9]. In this study we propose to design suitable formulations by incorporating lyophilized Cmn loaded solid lipid nanoparticles to form an in-situ gelling system for periodontal application. Further the antioxidant potential of Cmn loaded solid lipid nanoparticles is evaluated so as it can be used in management of periodontitis.

Materials and Methods

Materials

Cmn extract (95%) was a kind gift from Sunpure Extract Pvt Ltd.; India; Compritol® 888 ATO was a gift sample from Gattefosse;

France; and Phospholipon 90 G (soya lecithin) was gifted by Lipoid; Germany. Carbopol 934 was procured from Loba Chemie laboratory reagents and fine chemicals. Poloxamer 407 was gifted by BASF, Germany. Hydroxypropyl methylcellulose (HPMC E 5) was procured from Hyashibara Chemical; Mumbai; India. Pectin was procured from Herbstreith & Fox KG. Eudragit L 100 was procured from Evonik Industries, Germany. Sodium alginate and calcium chloride fused were procured from Central drug house, New Delhi. All reagents used in the research work were of analytical standard grade.

Methods

Preparation of Cmn loaded solid lipid nanoparticles (C-SLNs): Cmn SLNs were prepared using pre optimized formula by high pressure hot homogenization technique as shown in (Figure 1) [9;10]. Cmn (0.6% w/w in the final formulation) was dissolved in polyethylene glycol (PEG) 600 followed by addition of molten Compritol® 888 ATO. A primary crude emulsion was prepared by emulsifying this hot lipid phase with the aqueous surfactant phase containing Tween 80 and Phospholipon 90G (soya lecithin) maintained at a temperature 5-10°C above melting point of Compritol® 888 ATO (70°C to 75°C) using high-speed stirrer (Wise Tis HD 15D; Germany) at 8;000 rpm for 8 min. The coarse emulsion was subjected to high-pressure homogenization (HPH) using Emulsiflex C3 Avestin (Canada) homogenizer at 1000 bars and three cycles. The dispersion thus obtained was allowed to cool to room temperature, forming lipid nanoparticles by recrystallization of the hot dispersed lipid.

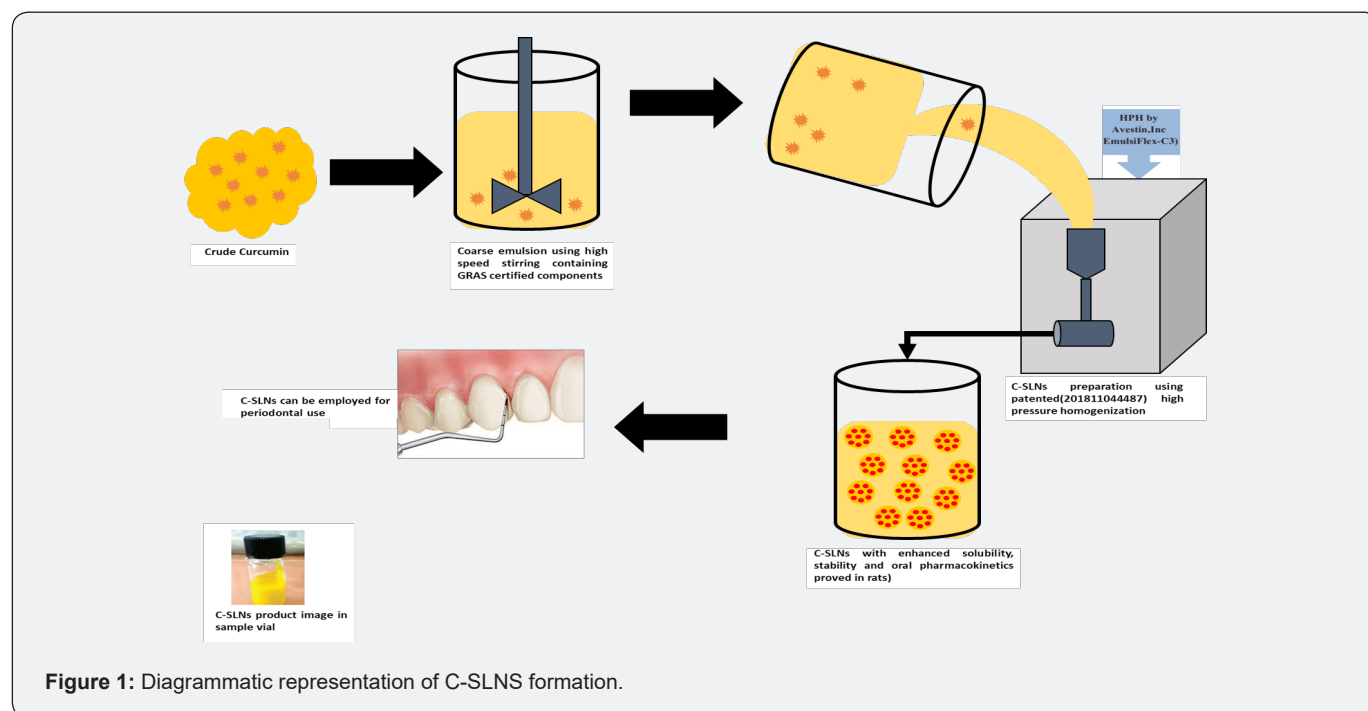


Figure 1: Diagrammatic representation of C-SLNS formation.

Lyophilization of prepared C-SLNs: The prepared C-SLNs were weighed; and mannitol was added (15% w/w) to it as a cryoprotectant. The mixture was frozen overnight and then

lyophilized for 2 cycles in lyophilizer (Alpha 2-4 LD plus) to obtain dry and free flowing C-SLNs as diagrammatically represented in (Figure 2).

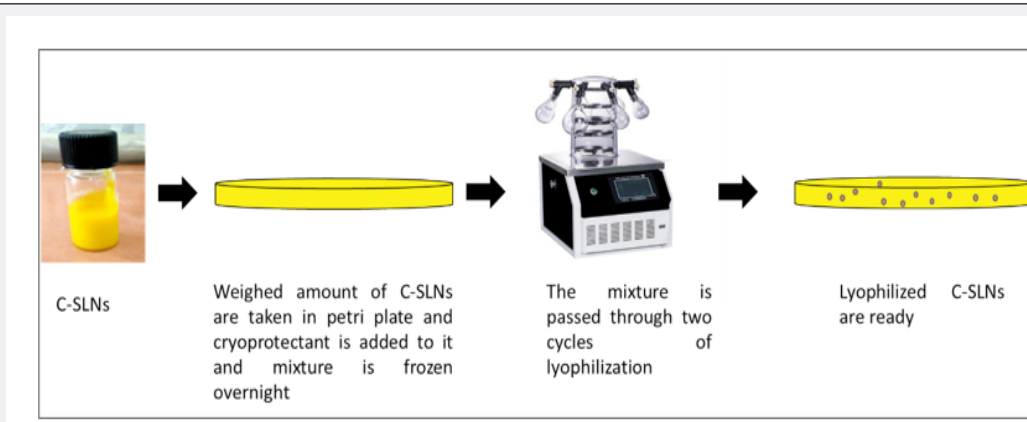


Figure 2: Diagrammatic representation of lyophilization.

Preparation of in-situ gelling system: Carbopol–poloxamer gel of C-SLNs was prepared by the cold method [11]. Carbopol 934 was first dissolved in deionized water over a magnetic stirrer at room temperature. Following complete dissolution; the solution was cooled in an ice bath and poloxamer 407 was added slowly to it with continuous stirring. The mixture was refrigerated at

40C for 24 h to ensure complete wetting/ solution and removal of entrapped air bubbles. lyophilized C-SLNS were added in small increments to the prepared polymer solution and mixed under high-speed stirring (WiseTis HD 15D; Germany) at 5000 rpm for 10 minutes. The scheme is represented in (Figure 3). The prepared gel was transferred into amber bottles and stored in refrigerator.

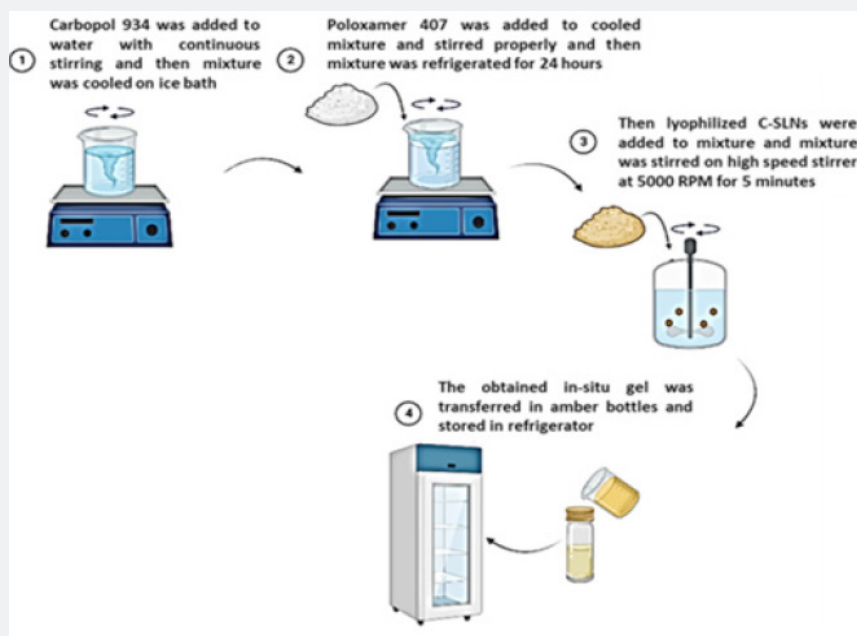


Figure 3: Diagrammatic representation of in-situ gelling system formation.

Spectrophotometric method for Cmn analysis: Standard plot of Cmn was prepared by validated method previously used in our lab [9]. Stock solution of 100ug/ml of Cmn was prepared (n=6) in in methanol:water (1:1). and diluted to obtain concentrations ranging from 1.0µg/ml to 7.0 µg/ml, which were then analyzed

spectrophotometrically at λ max of 425nm using methanol: water (1:1) as blank. The observed absorbance was plotted against corresponding concentration to obtain a straight line. The extinction coefficient; E1%1cm of Cmn was then calculated.

Characterization of prepared in-situ gelling systems

Determination of drug assay (total drug content [TDC]):

A weighed amount of the gel was dissolved in 10 mL methanol. The solution was then analyzed at a wavelength of 425 nm spectrophotometrically and methanol was kept as blank. Total drug content in the formulation was calculated using below mentioned equation:

$$\text{Total drug content (\%)} = \frac{\text{Observe drug content}}{\text{theoretical drug content}}$$

Particle size and polydispersity index (PDI): The mean particle size and PDI of in-situ gelling system (n=6) analysis was carried out after diluting the samples (100 times) with double distilled water. Instrument for analysis was Delsa™ Nano C Particle Analyzer (Beckman Coulter; USA).

Determination of pH: The pH of in-situ gelling system was determined using a calibrated pH meter at 4°C. The readings were taken for an average of 6 samples.

Syringe ability study: The ability of the prepared formulations to flow easily through a syringe of 21-gauge needle was assessed using the reported method [12]. One ml of the cold gel was filled in 21-gauge needle syringe and the ability of the gel to flow under normal handling pressure was assessed.

Gelation temperature: For the measurement of gelation temperature; 10 ml sample was taken and placed in 20 ml beaker. A magnetic stirring bar was placed in the beaker. The temperature of the sample was increased gradually at the rate of 1°C /min and the temperature at which the movement of the magnetic bar was hindered was recorded as the gelation temperature [13]. Alternatively, the gelation temperature was also determined using the test-tube inverting method. A volume of 2 ml of the in-situ gel was placed in a test tube, which was then immersed in a water bath at 15°C. The temperature of the water bath was then gradually increased; samples were examined every 2 minutes; and the gelation temperature was recorded when the gel stops flowing upon test tube inversion at 90°. The readings were taken for an average of 6 samples [14].

Texture analysis of in-situ gelling system: The mechanical property of in-situ gelling system was determined using a software-controlled penetrometer; texture analyzer (Stable Micro systems; Surrey; UK). The formulation was transferred to a bottle and kept in an ultrasonic water bath to remove air bubbles for 20min and the temperature was adjusted to 37°C. The probe was compressed into the CSLN in situ gel at a defined rate of 2mm s⁻¹. Various mechanical parameters such as hardness; compressibility; adhesiveness; and cohesiveness of the gel formulation were estimated.

Rheological evaluation: The rheological properties of prepared in-situ gelling systems were measured using Rotational Rheometer (Model Rheolab QC from Anton Paar; Austria).

Differential scanning calorimeter (DSC): DSC thermograms of Cmn; lyophilized C-SLNS; prepared in-situ gelling system and blank gel were taken using Q20 differential scanning calorimeter instrument. Hermetic pans were used for analysis that was heated at a rate of 10°C/min covering the range of 30 to 300°C. This analysis is carried out in nitrogen atmosphere.

Fourier transform infra-red (FTIR): FTIR spectra of Cmn; lyophilized C-SLNS; prepared in-situ gelling system and blank gel were taken using KBr pellet technique. Instrument used was 60MHz Varian EM 360 (Perkin Elmer; USA). The peaks obtained after the sample run were evaluated for any significant changes.

In vitro drug release: One ml of gel was filled in dialysis bag which was then tied from both ends. Bag was then suspended in 50 ml of methanol: water (1:1) preheated at 37 ± 0.5°C in shaking water bath at maintained 37°C and 80rpm. At predetermined time intervals, 2 mL sample was withdrawn and replaced with an equal volume of fresh medium. Samples were diluted and analysed using an UV spectrophotometer for Cmn concentration at λ max 425 nm. The cumulative amount of drug released was calculated based on a calibration curve of Cmn in methanol: water (1:1). All experiments were done in hexaplicates.

DPPH in vitro antioxidant assay kinetics

DPPH calibration curve: A stock solution of 2.54 × 10⁻² mM of DPPH (2; 2-diphenyl-1-picrylhydrazyl) was prepared; and serial dilutions were made to obtain six dilutions with concentrations of 1.27 × 10⁻²; 6.35 × 10⁻³; 3.18 × 10⁻³; 1.59 × 10⁻³; 7.95 × 10⁻⁴; and 3.98 × 10⁻⁴ mM. The absorbance of the various concentrations was measured at a wavelength of 517 nm; being the wavelength of maximum absorbance using a UV-vis spectrophotometer; subsequently generating a graph of absorbance against concentration (calibration curve); where the slope of the graph represents the molar absorptivity (ε) of DPPH according to the Beer-Lambert law.

DPPH scavenging activity: The antioxidant potential of Cmn; ascorbic acid and C-SLNS was determined based on their ability to scavenge the stable DPPH free radical adopting the methods of [15] with modifications. Stock solutions of Cmn; ascorbic acid and C-SLNS were prepared to obtain a concentration of 1000µg/mL. Dilutions were made to obtain concentrations ranging from 10-1000µg/mL; 2 mL of each of these dilutions were mixed with 2 mL of methanol solution of DPPH at a concentration of 0.0254 mM. The mixture was then vigorously shaken and allowed to stand in the dark at room temperature. The absorbance of the mixture was measured at various time intervals at 517 nm with a mixture of methanol and DPPH solution used as control. The absorbance results were obtained in triplicate; and the average values were used as the actual absorbance. The scavenging activity of the DPPH radical can be expressed as inhibition percentage using the following equation according to [15].

$$\% \text{inhibition} = \frac{AB - AS}{AB}$$

where AB is the absorbance of the control (containing all reagents except the test compound); and AS is the absorbance of the mixture with the test compound. The IC₅₀ value of the samples; which is the concentration of a sample required to inhibit 50% of the DPPH free radical; was calculated from the graph of percentage inhibition against extract concentrations.

Kinetic analysis: At different time intervals; the concentrations of the DPPH radical in the mixture samples were calculated using the Beer-Lambert law

$$A = \varepsilon cl$$

Integration method

$$-d \frac{[DPPH]}{dt} = -k_2 [DPPH]^2$$

Then an integrated form of this type of second-order reaction rate equation was applied to the experimental results.

$$E^{10} \log \frac{[DPPH]_0}{[DPPH]_t} = k_2 t$$

where {DPPH}₀ and {DPPH}_t are the DPPH concentrations at time zero and any time "t"; respectively. A plot of 1/{DPPH}t against time gives a slope k₂.

Isolation method

This may be applied to the kinetics of scavenging the free radical; DPPH; by a pseudo-first order means. This method of obtaining the kinetics of antioxidant activity was adapted from [16] using DPPH and antioxidant concentrations of the mixture samples.

$$-d \frac{[DPPH]}{dt} = k_2 \{DPPH\} \{antioxidant\}$$

The second-order rate constant (k₂) was determined by having the concentration of the antioxidant; {antioxidant}; to be in large excess compared to the concentration of the radical compound {DPPH}. This forces the reaction to vary only with the concentration of DPPH.

$$-d \frac{[DPPH]}{dt} = k_1 (DPPH)$$

$$\text{Where; } k_1 = k_2 \{antioxidant\}$$

{antioxidant} is assumed to remain constant throughout the reaction and can be modified to obtain different k₁ values. The change in {DPPH} with time gives k₁. Determination of k₁ was repeated at different antioxidant concentrations for each of the samples; and the mean gave the overall k₁. We can; therefore; infer that DPPH was depleted from the medium under pseudo-first-order conditions according to the following equation:

$$\{DPPH\}_t = \{DPPH\}_0 e^{-k_1 t}$$

where {DPPH}t represents radical concentration at any time (t); {DPPH}0 corresponds to concentration at time zero; and k₁ is a constant for pseudo-first-order rate. This rate constant (k₁) is linearly dependent on the concentration of the antioxidant; and from the slope of these plots; k₂ was determined.

Results and Discussion

Formulation development of in-situ gelling systems

In-situ gel-forming formulations help deliver drugs as a liquid dosage form; which then form strong gels after application at delivery site; thus, prolonging the residence time of the active substance [17]. Amongst in-situ gelling polymers; thermosensitive systems containing poloxamer have been investigated as a convenient dosage form for application into periodontal pocket [18]. Furthermore, semisolid formulations consisting of mucoadhesive polymers such as sodium alginate; polycarboxiphil; hydroxypropyl cellulose; polyvinylpyrrolidone; and carbopol have been proposed to improve the intimacy of contact and increase the residence time of the dosage form in the periodontal pocket. Based on these observations we chose poloxamer 407 and carbopol 934 presently for the proposed situ gelling system. Various formulations of in situ gelling systems were prepared in lab incorporating 40g of lyophilized C-SLNS (equivalent to approx 6mg per ml of Cmn/6mg per g of gel). The formulations were contained poloxamer 407 ranging from 5-30% and carbopol 934 ranging from 0.25-1% (Table1; Figure 4,5,6). Characterization of the developed in-situ gelling systems was done in terms of release behavior; physical stability; viscosity; and syringe ability to identify the most suitable formulation. Formulation F1 and F2 were very viscous and exhibited poor syringe ability (Table 2). Further negligible amount of Cmn was released from them in initial 4-5 h (they exhibited a lag period of > 4-5 h). In contrast formulations F3, F4 and F5 showed optimum viscosity; were easily syringe able and showed good release characteristics. Formulation F4 showed sustained release up to 8 days whereas formulation F3 and F5 did not exhibit sustained release.

Table 1: Composition of in-situ gelling systems.

Formulation Code	Poloxamer 407(%w/w)	Carbopol 934(%w/w)
F1	30	1
F2	15	1
F3	10	1
F4*	10	0.5
F5	5	0.25

Spectrophotometric method for Cmn analysis

Cmn was spectrophotometrically analysed at λ max of 425nm and a standard curve (Figure 7) of Cmn was prepared in the range of 1-7 μ g/mL in agreement with Beer-Lambert's Law (Table 3).

Characterization of prepared in-situ gelling systems

Determination of drug assay (total drug content [TDC]):

The TDC of in-situ gelling system was found to be 5.82 \pm 0.14 mg/ml (97.00 \pm 0.01%) (n=6).

Table 2: Characterization of various formulations of in-situ gelling systems.

Formulation Code	Release behaviors (hours/days)	Physical Stability	Viscosity	Syringe ability
F1	lag period > 5h	****	**	**
F2	lag period > 4h	****	***	***
F3	8 days (not sustained)	****	****	****
F4+	8 days (sustained)	*****	*****	*****
F5	6 days (not sustained)	*****	*****	*****

*****Good stability/less viscosity/easily syringeable, *least stability/high viscosity/difficult to syringe, +Most optimum formulation. Based on the characterization tests described above in Table 2, formulation F4 was selected for further development.

Table 3: Spectrophotometric analysis of Cmn (n=6).

Solvent	$E^{1\% 1cm}$	y=mx	R2
methanol: water (1:1)	1186	0.1186x	0.9973



Figure 4: Image of in-situ gelling system at 37°C.



Figure 5: Image of in-situ gelling system when taken out from fridge.

Particle size and polydispersity index (PDI) analysis: The average particle size of C-SLNs was 576.4 ± 45.1 nm and a significantly low PDI of 0.237 ± 0.026 was observed (n=6; Figure

8). A low PDI indicates a uniform distribution of particles around the mean.



Figure 6: Image of in-situ gelling system when kept at room temperature for some time.

Determination of pH: The pH of in-situ gelling system was 7.2 ± 0.5 (n=6). Cmn is unstable at acidic and alkaline pH and the optimal pH should be between 6.2 to 7.4. The pH of in situ gel formulation should be such that Cmn is stable at that pH and at the same time patient should not experience any irritation or discomfort upon application. The developed in-situ gel formulations showed an optimal pH.

and passed with ease through 24-gauge needle at 4°C.

Gelation temperature: Gelation temperature of the formulation indicates the temperature at which the formulation undergoes phase conversion from liquid to solid. The gelation temperature of the prepared optimal formulation $32 \pm 0.9^\circ\text{C}$ (magnetic bead method) and $34 \pm 0.6^\circ\text{C}$ (inverted test tube method).

Syringeability study: The gelling system was syringe able

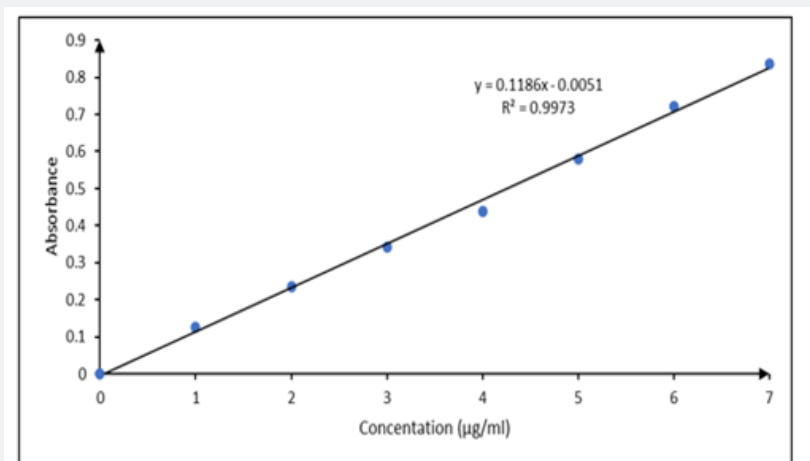


Figure 7: Standard plot of curcumin in methanol: water.

Texture analysis of in-situ gelling system: Texture profile analysis (TPA) is used to evaluate mechanical properties of the developed formulation i.e., in-situ gel. It tells about the physical structure of the formed gel. Basically, it predicts the behavior of

the sample when placed under varied storage and physiological conditions. Various parameters viz; compressibility; hardness; adhesiveness; and elasticity can be determined using TPA. The altitude of the first peak in the graph is indicative of hardness

value which is basically the force required to attain a given level of deformity. It is represented as positive peak in the graph; and it talks about the applicability of the gel to the application site. In general, more is the hardness value of the sample; better will be its consistency. As a rule, hardness increases on increase in the polymer concentration. The maximum force attained on the graph is a measure of the firmness of the sample at the specified depth (hardness). The maximum negative force was taken as an indication of the stickiness/cohesiveness of the sample. The work required to deform the gel in down movement of probe indicates

cohesiveness. The adhesiveness of the sample is defined as amount of work required to surpass the attractive forces prevalent in-between the surfaces of the sample and the contacting surface of the probe. Hardness of the optimized formulation was 873.66 g (Table 4; Figure 9). It represents a negative peak in the graph and highlights the proper contact to the application site. It is indicative of enhanced bioavailability of the drug formulation. Adhesiveness value of the optimized formulation from the TPA analysis came out to be -714.27 g. sec (Table 4; Figure 9).

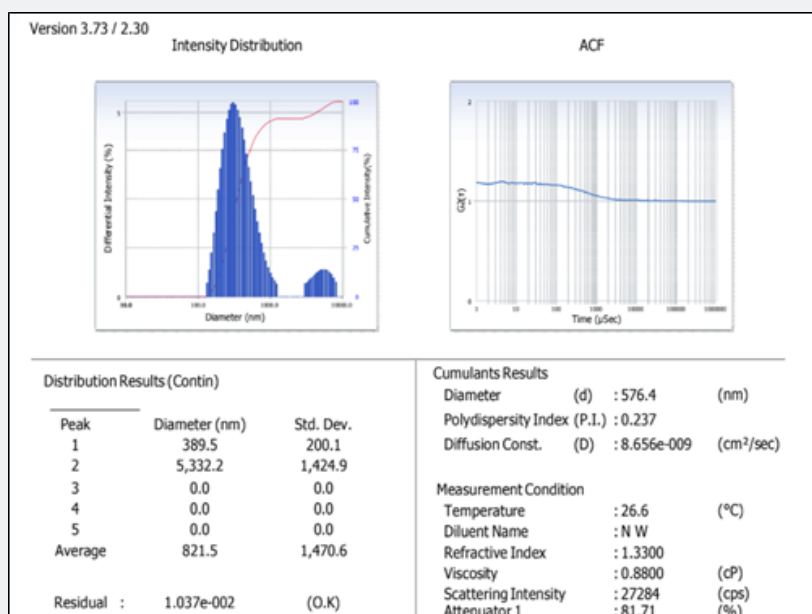


Figure 8: Particle size of in-situ gelling systems.

Table 4: Texture profile analysis.

Test ID	Firmness	Consistency	Cohesiveness	Work of Cohesion
	g	g. sec	g	g.sec
	Force 1	Area F-T 1:2	Force 2	Area F-T 2:3
Gell	873.66	792.68	-430.2	-714.27

Rheological evaluation: Developed optimal gel formulation showed characteristic pseudoplastic flow with thixotropy. The analysis showed shear thinning phenomenon, which is good for the developed periodontal gel (Figure 10). This characteristic behavior allows the molecules present in the sample to remain entangled in the immobilized solvent. When shear is applied; the molecules disengaged themselves and get aligned into the direction of the flow. This results in lesser resistance to the flow and allows the release of entrapped water which corresponds to the lower viscosity of the developed system. The analysis proved that there was decrease in viscosity with increase of shear rate which is the characteristic feature of the non-Newtonian pseudoplastic behavior. The viscosity of in situ gelling system was 241000000 mPa.s at 37°C.

Differential scanning calorimeter (DSC): DSC is a thermo-analytical technique which is based on the principle for the differences in the amount of heat required to keep sample as well as reference standard at same temperature. The reading is noted as the function of temperature and time. In case of pure Cmn (Figure 11); a melting endotherm appeared at 176.89°C (247.8 J/g) corresponding to its melting point at 180-183°C. In case of lyophilized C-SLNs and the corresponding gel; the peak shifted to a lower temperature of 168.38°C and 167.59°C; respectively. Since, melting endotherm of Cmn in all these thermograms were in a close range; so it is concluded that the drug remains in the same state; in lyophilized C-SLNs and in the in-situ gelling system formulation and there is no interaction with polymers used in the formulation of latter (Figure 12-14).

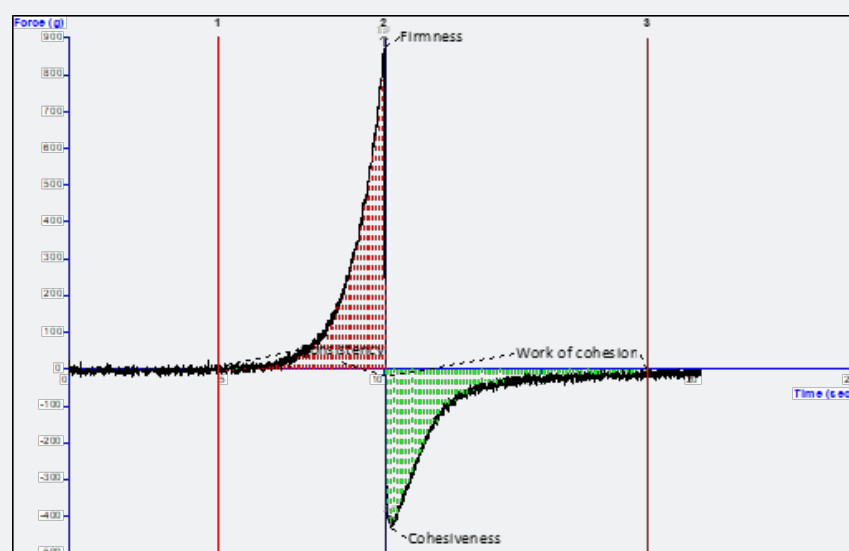


Figure 9: Graph showing cohesiveness, consistency, firmness and work of cohesion of in-situ gelling system.

Fourier transform infra-red (FTIR) studies: FTIR spectra for pure Cmn; lyophilized C-SLNs; blank gel and in-situ gelling system are depicted in (Figure 15-18). For Cmn (Figure 15); the sharp peak at 3512 cm^{-1} attributes to the phenolic O-H stretching vibration. The bands at 1628.60 cm^{-1} and 1514.40 cm^{-1} are related to carbonyl group C = O and stretching vibrations of the benzene ring, respectively. The bands at 1428.80 cm^{-1} are related to olefinic bending vibration of C-H bound to the benzene ring of Cmn. The bands at 1280.40 cm^{-1} are due to aromatic C = O stretching. The 1514.4 cm^{-1} ring peak is assigned to the (C=O); while enol C-O peak was obtained at 1280.40 cm^{-1} ; C-O-C stretching vibrations at 1029.30 cm^{-1} and benzoate trans-CH vibration at 960.81 cm^{-1} . Further, absence of characteristic peaks of Cmn in the IR spectrum

of the lyophilized C-SLNs (Figure 16); indicate encapsulation of Cmn in the SLNs. Observation of broad absorption peak of OH at 3287.18 cm^{-1} in the FTIR spectrum of CSLNs (Figure 16) suggest that this peak is due to PEG 600 as also reported. IR spectrum of poloxamer 407 is characterized by principal absorption peaks at 2926.87 cm^{-1} (C H stretch aliphatic); 1298.30 cm^{-1} (in plane O H bend); and 1095.53 cm^{-1} (C O stretch) shown in (Figure 17). IR spectrum of Carbopol 934 is characterized by principal absorption peaks at 2926.87 cm^{-1} (O H stretching); 1644.84 cm^{-1} (carboxyl group) shown in (Figure 17). The interaction between the drug and the polymers often leads to identifiable changes in the FTIR profile of solid systems. The spectrum of in-situgelling system was equivalent to the spectrum of pure drug, indicating no interaction.

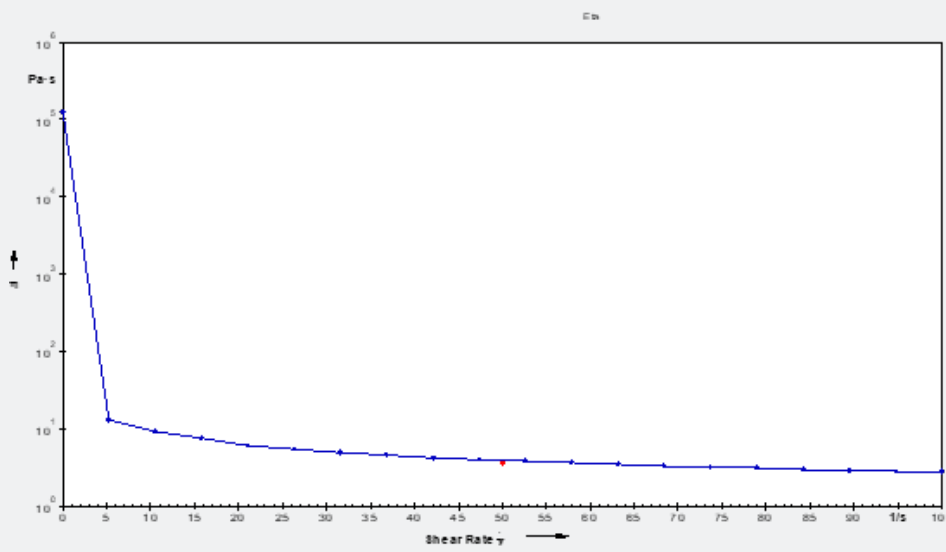


Figure 10: Viscosity v/s shear rate curve for in situ gelling system at 37°C .

In vitro drug release: The release media for Cmn was selected keeping in mind its insoluble nature and tendency towards degradation in buffer solution. Cmn showed good solubility in methanol; so different proportions of methanol was mixed with solutions buffered to a pH ranging from 6.6-6.8 (as of gingival fluid). However, methanol precipitated electrolytes from the buffers. Further on trying with ethanol, electrolytes won't get precipitated; but Cmn gets degraded in this buffer solution. Hence ratio of methanol: water (1:1) was finalized as the release media. Different concentrations of methanol (10-50%) were tested prior to finalization but it was found that 50% in water was sufficient for Cmn dissolution and maintenance of sink conditions. The drug release from in-situ gelling system is shown below in (Figure 19).

The release from in-situ gelling system extended upto 8 days with 99.182 ± 0.02 % release and followed Higuchi kinetics (Table 5). This type of kinetics is exhibited by matrix type delivery systems wherein the active is uniformly distributed throughout the matrix and is released by diffusion and/or matrix dissolution or erosion [19].

DPPH in vitro antioxidant assay kinetics

DPPH calibration curve: Absorbance of varying concentrations of DPPH solution at 517 nm was determined to generate a calibration curve; thereby; assigning the molar absorptivity of DPPH (12.485). A linear regression (R^2 value) of 0.9902 was obtained from the curve (Figure 20).

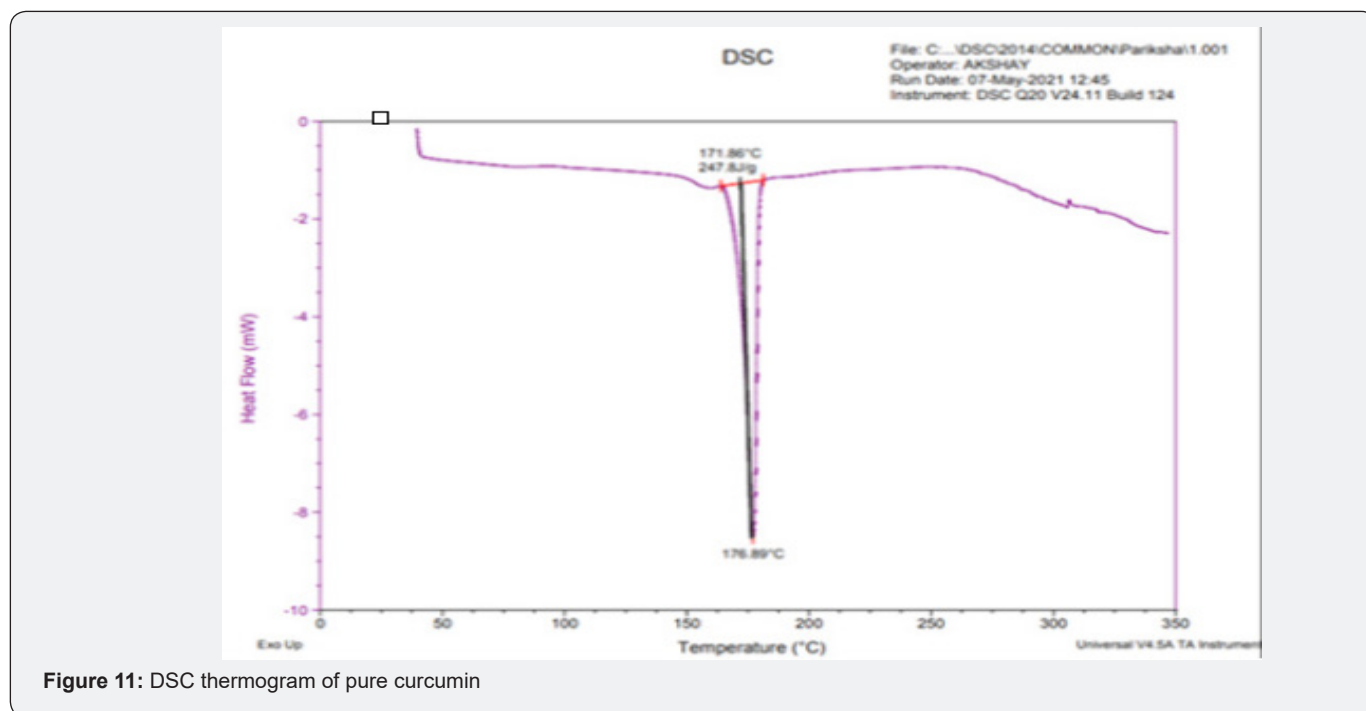


Figure 11: DSC thermogram of pure curcumin

Antioxidant activity: The % inhibition of DPPH by Cmn; ascorbic acid and C-SLNS (Figure 21-23) shows that all three have good inhibition ability at the experimental concentrations, although the inhibition ability of C-SLNS is stronger than that of Cmn and ascorbic acid. IC50 values of C-SLNS; Cmn and ascorbic acid are given and compared in (Table 6; Figure 24). Using one way ANOVA it was found that there was no significant difference in IC50 of ascorbic acid; Cmn and C-SLNS ($P < 0.05$) Figure 25. Although C-SLNS showed arithmetically higher IC50 during initial hours but it effects better than Cmn and ascorbic acid at later stages [20].

Integration method: The result of the second-order rate constant (k_2) of the free radical scavenging activities of ascorbic acid; free Cmn solution in methanol and C-SLNS by the integration method is summarized in (Figure 26-28). This result was obtained from a plot of $1/[DPPH]t$ vs time. The second-order rate constant; k_2 ; which is depicted by the slope of the plots; was averaged to obtain an overall second-order rate constant of the antioxidant activities of ascorbic acid; free Cmn solution

in methanol and C-SLNS. An average k_2 of 0.00278; 0.00293 and 0.00392 ($\text{mM}^{-1} \text{min}^{-1}$) were obtained for ascorbic acid; free Cmn solution in methanol and C-SLNS respectively. This observation of a higher k_2 in C-SLNS leads to the inference that C-SLNS scavenges the DPPH radical faster than Cmn and ascorbic acid at the same concentration. The R^2 values of the trend lines over all concentrations were averaged to obtain the overall R^2 values in each case. The values are 0.6897; 0.7225 and 0.8798 for ascorbic acid; Cmn and C-SLNS respectively.

Isolation method: Different pseudo-first-order rate constants (k_1) were obtained according to equation:

$$-d \frac{[DPPH]}{dt} = -[DPPH]^2$$

whose integrated form leads to

$$\ln \frac{[DPPH]_t}{[DPPH]_0} = -k_1 t$$

$$\ln \frac{[DPPH]_t}{[DPPH]_0}$$

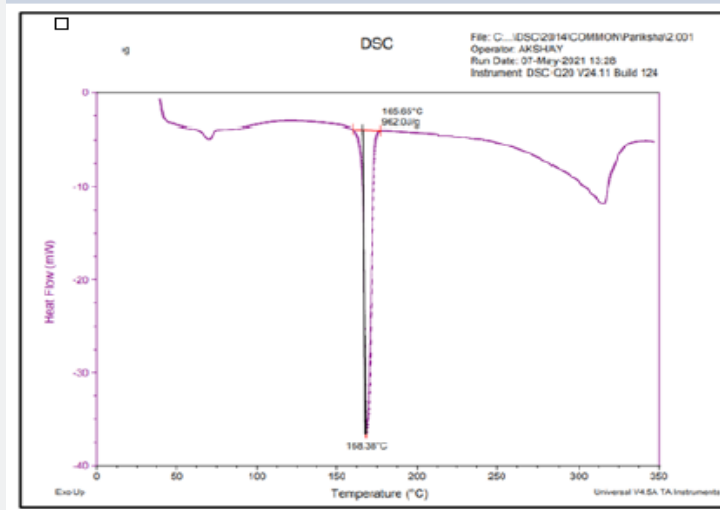


Figure 12: DSC thermogram of lyophilized C-SLNS.

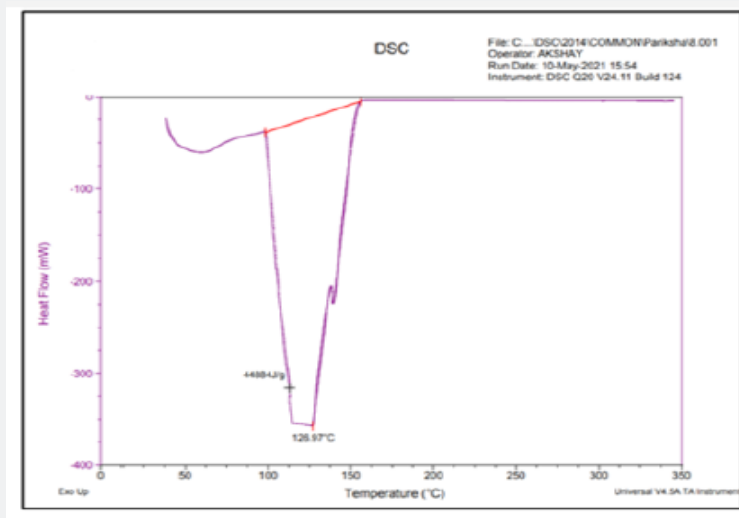


Figure 13: DSC thermogram of blank gel.

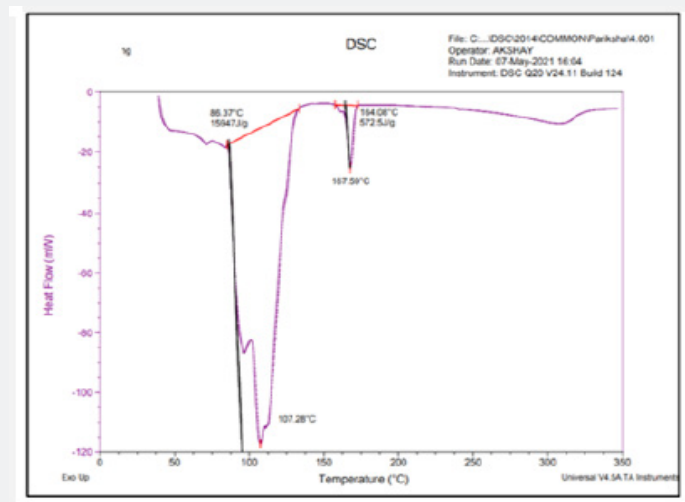


Figure 14: DSC thermograms of in-situ gel.

Table 5: Release models.

S.no	Model	Slope	Intercept	Regression Coefficient
1	Zero order	0.526	3.763	0.977
2	First order	-0.007	2.045	0.808
3	Higuchi	7.024	-6.127	0.983
4	Hixson Cronwell	-0.016	4.622	0.944
5	Kornsmeier	0.664	0.407	0.97

Table 6: IC50 of Ascorbic acid, free Cmn solution in methanol and C-SLNS at various time points.

Time (min)	Ascorbic Acid	Cmn	C-SLNS
	IC50(mM)	IC50(mM)	IC50(mM)
30	814.72±0.20	877.47±0.10	1574.70±0.21
50	747.08±0.22	774.77±0.05	1295.68±0.19
70	668.89±0.12	675.07±0.20	973.05±0.12
90	567.25±0.17	569.10±0.06	909.62±0.06
360	412.31±0.09	427.48±0.07	654.22±0.05
1440	316.92±0.07	318.10±0.08	497.87±0.15
2880	296.35±0.17	296.38±0.12	372.88±0.14
4320	275.64±0.16	270.47±0.15	290.42±0.12
5760	255.76±0.08	248.26±0.07	229.36±0.10
7200(= 5 days)	233.69±0.06	217.65±0.09	152.12±0.20

Therefore, a plot of k_2 against times (t) gave a slope equal to $-k_1$ (Figure 29-31). The linear relationship between k_1 and the concentration of the compounds; $k_1=k_2$ (antioxidant) allows us to obtain k_2 from the slope of their respective graphs. The second-order rate constants (k_2) obtained from the pseudo-first-order rate reaction are 0.000052; 0.000054 and 0.000073 (mM)⁻¹ min⁻¹ for ascorbic acid; free Cmn solution in methanol and C-SLNS

respectively. This observation of a higher k_2 in C-SLNS confirmed the inference that C-SLNS scavenges the DPPH radical faster than Cmn and ascorbic acid at the same concentration. The linear regression coefficient (R^2) of 0.8228 for C-SLNS revealed that it is more favored in the pseudo-first-order kinetics than ascorbic acid and Cmn with a regression coefficient of 0.6531 and 0.6846 respectively.



Figure 15: FTIR spectra of pure curcumin.

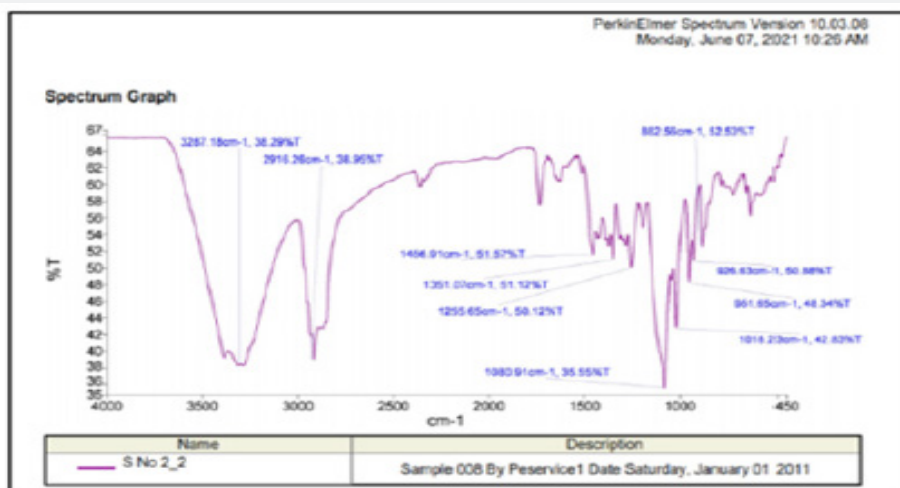


Figure 16: FTIR spectra of lyophilized C-SLNS.

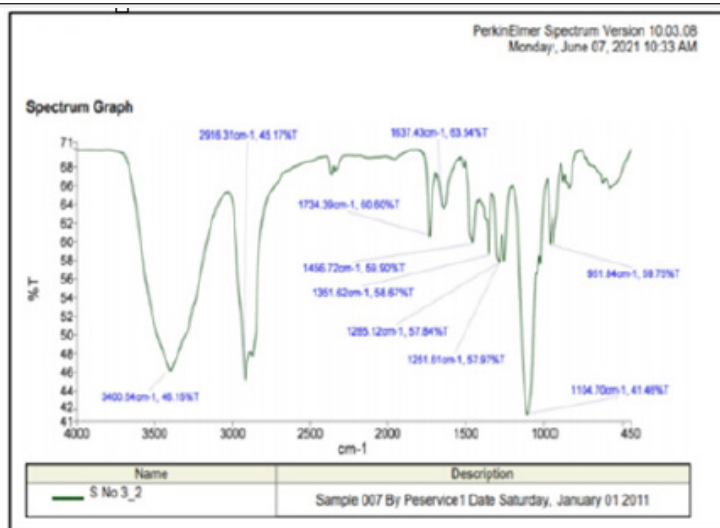


Figure 17: FTIR spectra of blank gel.

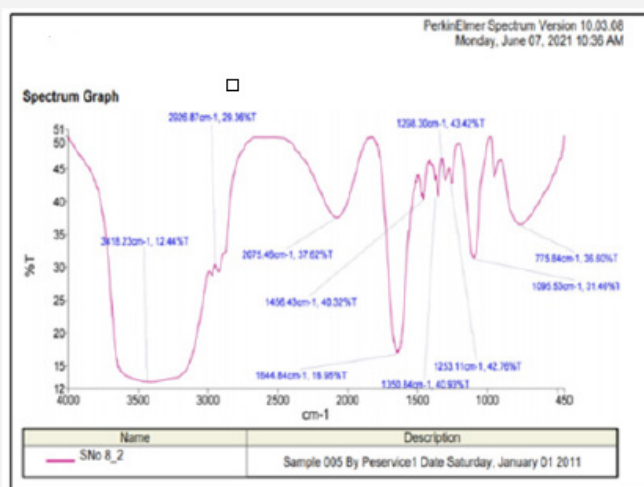


Figure 18: FTIR spectra of in-situ gel.

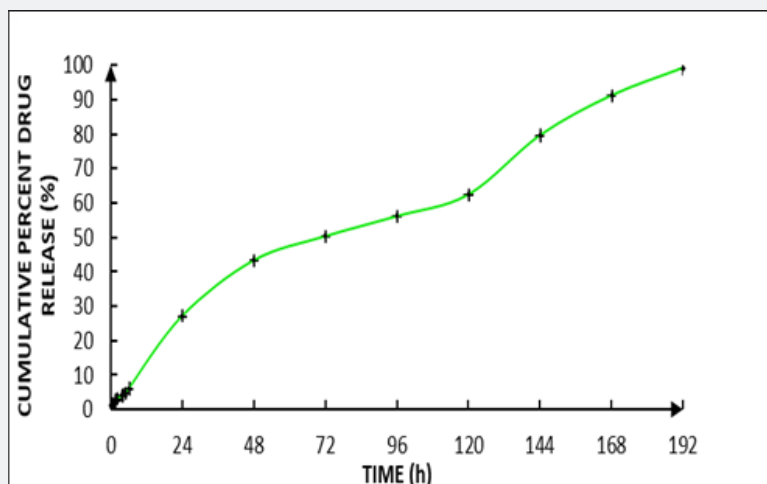


Figure 19: Cumulative percent release (%) versus time(h) graph for in-situ gelling system.

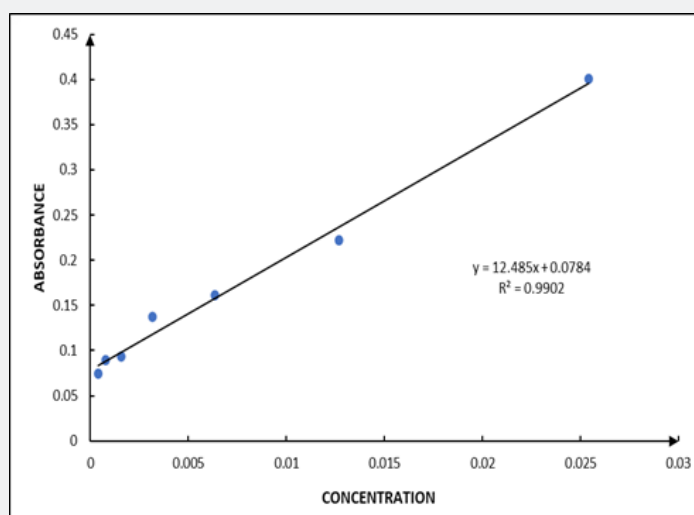


Figure 20: Standard plot of DPPH in methanol.

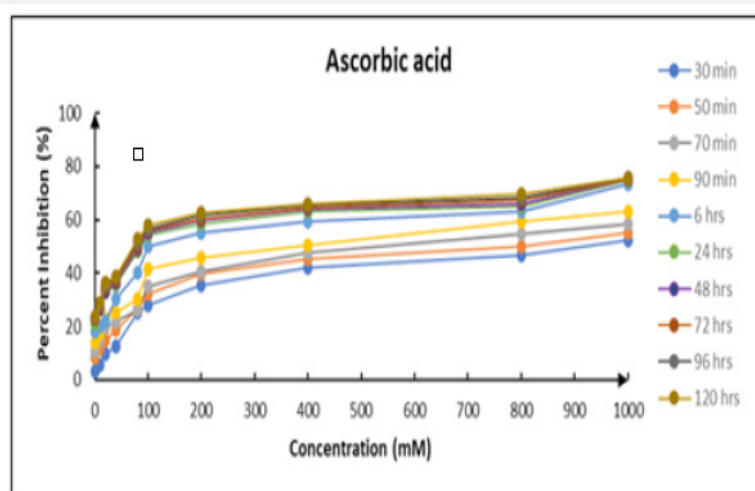


Figure 21: Percent inhibition of DPPH versus concentration graph at various time points for ascorbic acid for determination of the second-order rate constant.

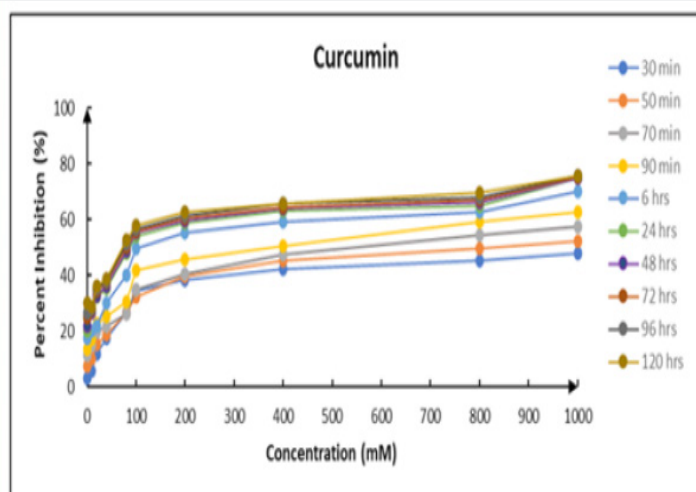


Figure 22: Percent inhibition of DPPH versus concentration graph at various time points for free curcumin solution in methanol for determination of the second-order rate constant.

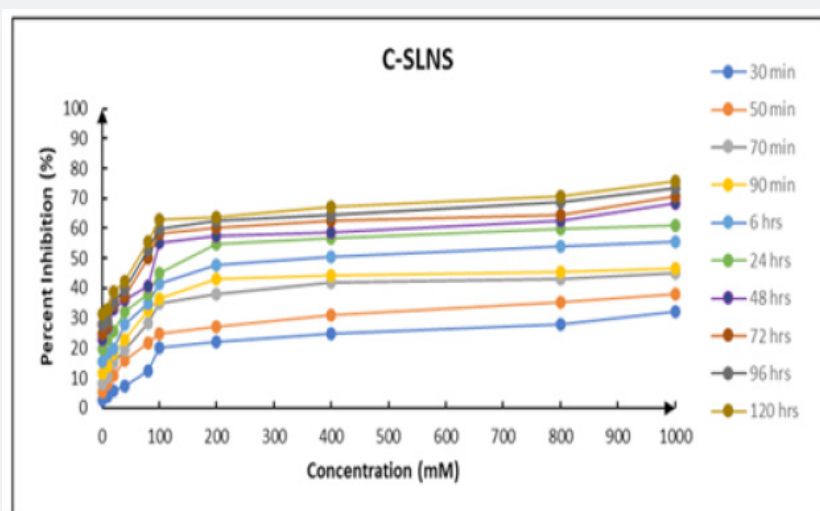


Figure 23: Percent inhibition of DPPH versus concentration graph at various time points for C-SLNs for determination of the second-order rate constant.

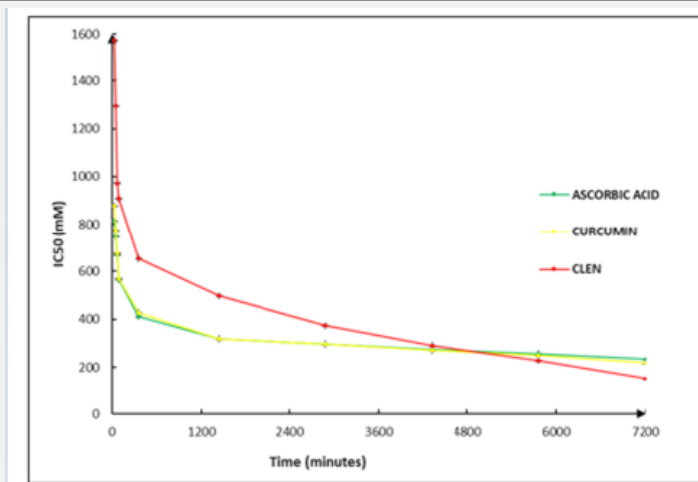


Figure 24: IC₅₀(mM) versus time (min) graph for ascorbic acid, free curcumin solution in methanol and C-SLNS in DPPH assay. IC₅₀ Values for all three treatments were similar at all time points (P<0.05).

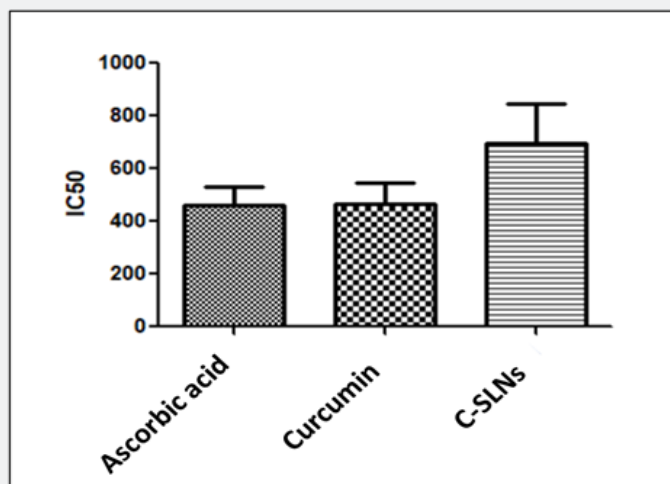


Figure 25: Comparison of mean IC50 values for Ascorbic acid, free curcumin solution in methanol and C-SLNs in DPPH assay.

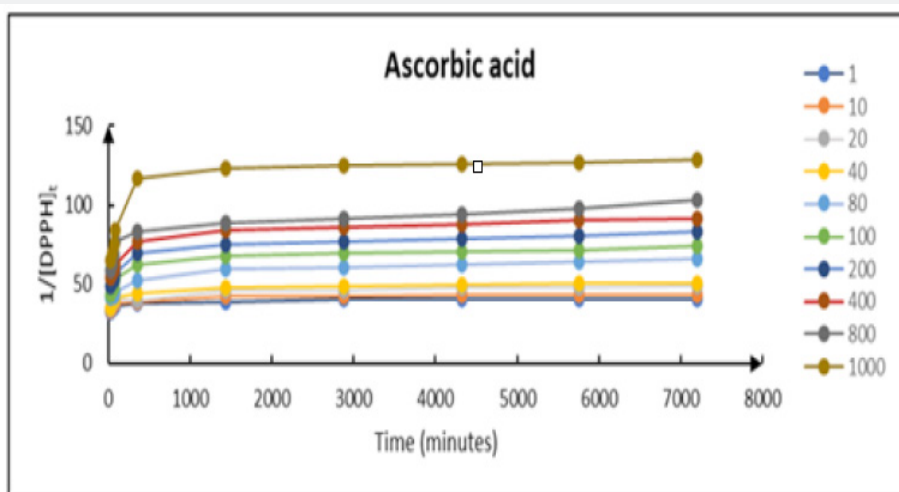


Figure 26: $\ln \frac{[DPPH]_t}{[DPPH]_0}$ time graph at various concentrations for ascorbic acid for determination of the second-order rate constant.

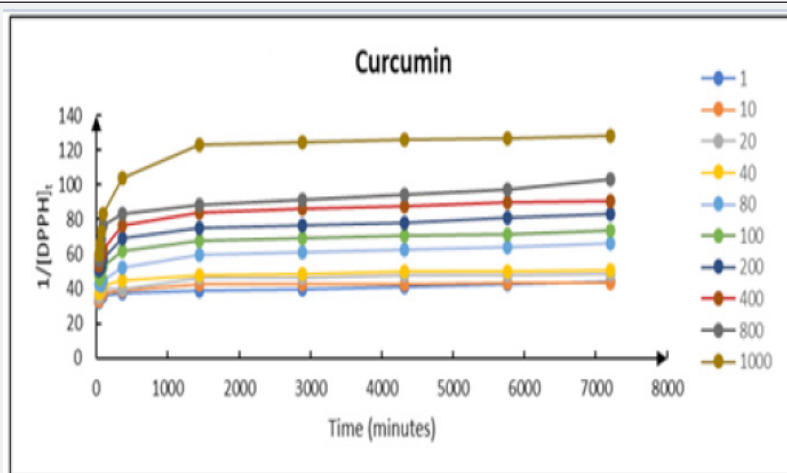


Figure 27: $\frac{1}{[DPPH]_t}$ time graph at various concentrations for free curcumin solution in methanol for determination of the second-order rate constant.

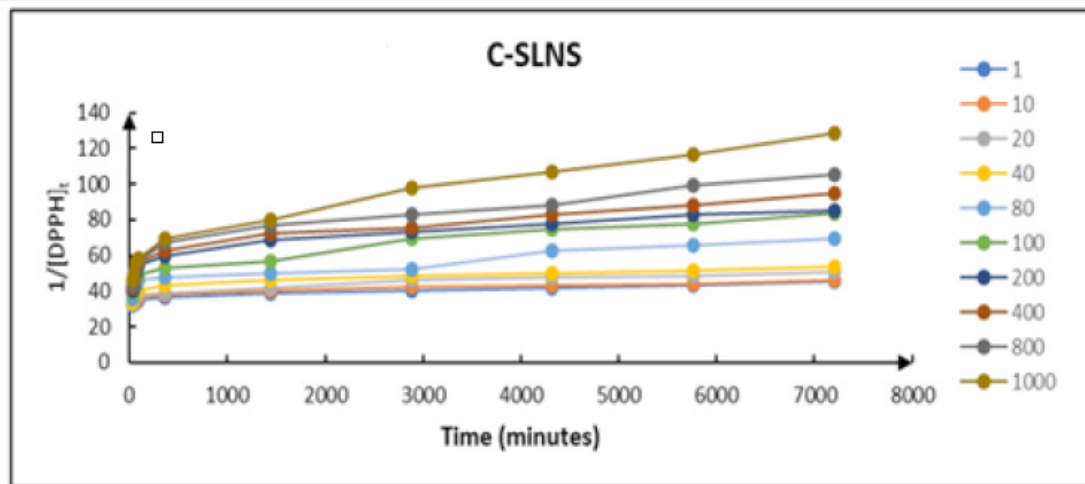


Figure 28: $\frac{1}{[DPPH]_t}$ time graph at various concentrations for C-SLNS for determination of the second-order rate constant.

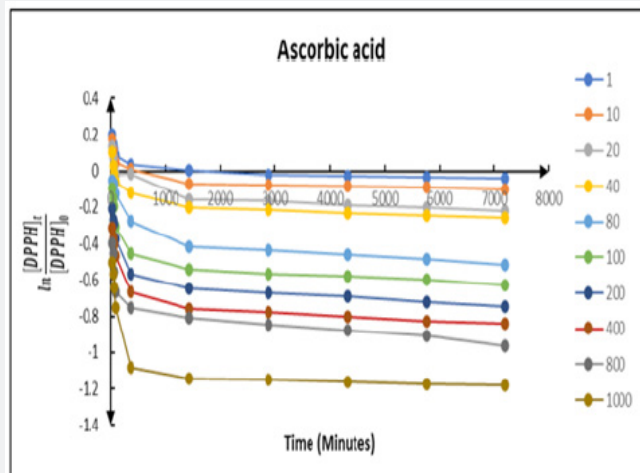


Figure 29: $\ln \frac{[DPPH]_t}{[DPPH]_0}$ time graph at various concentrations for ascorbic acid for determination of $-k_1$.

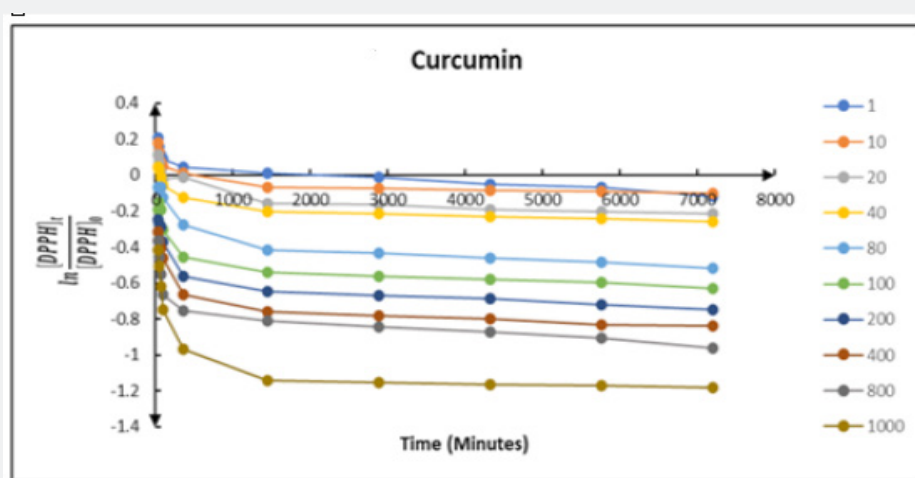


Figure 30: $\ln \frac{[DPPH]_t}{[DPPH]_0}$ time graph at various concentrations for free curcumin solution in methanol for determination of $-k_1$.

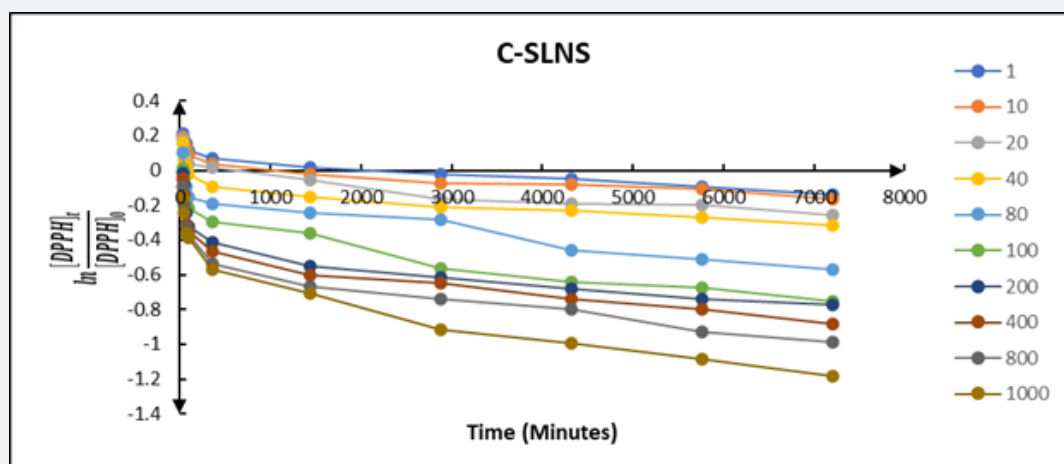


Figure 31: $\ln \frac{[DPPH]_t}{[DPPH]_0}$ v/s time graph at various concentrations for C-SLNS for determination of $-k_1$.

Conclusion

Local delivery of Cmn in the form of site-specific periodontal formulations can open newer option for the management of periodontal diseases. Efficacy of such delivery systems is dependent on the sustained release of Cmn from the device in a soluble form and its penetration into the base of the periodontal pocket and adjacent connective tissue. In the study, we have prepared periodontal formulations incorporating C-SLNs a previously established soluble; stable; and bioavailable form of Cmn. In-situ gelling systems showed a prolonged and sustained release up to 8 days (192h). This shows that Cmn has good compatibility with temperature sensitive polymer poloxamer depicting a favorable release profile. Further superior antioxidant potential of C-SLN was established in comparison with free Cm and ascorbic acid. This was evident due to the slow release of Cmn from the SLNs. Thus, the study highlighted the antioxidant action of Cmn in the developed in-situ gelling system that can be exploited in the better management of periodontitis.

Declaration of Competing Interest

There are no conflicts of interest.

Acknowledgement

Joga Singh is supported by the ICMR Senior Research Fellowship; New Delhi (45/78/2018-NAN/BMS). Garima Sharma is funded by DST SERB; CII (New Delhi) and Hitech Formulations Pvt Ltd (Chandigarh); under Prime Minister Fellowship scheme (DST/SSK/SERB-CII-Fell/2014).

References

- Xu W, Zhou W, Wang H, Liang, S (2020) Roles of Porphyromonas gingivalis and its virulence factors in periodontitis. *Advances in Protein Chemistry Structural Biology* 120: 45-84.
- Kapoor A, Malhotra R, Grover V, Grover D (2012) Systemic antibiotic therapy in periodontics. *Dental Research Journal* 9: 505.
- Muglikar S, Patil, KC, Shivswami, S, Hegde R (2013) Efficacy of curcumin in the treatment of chronic gingivitis: a pilot study. *Oral Health & Preventive Dentistry* 11: 81-86.
- Kohli K, Ali J, Ansari M, Raheman Z (2005) Curcumin: a natural antiinflammatory agent. *Indian Journal of Pharmacology* 37: 141.
- Jurenka JS (2009) Anti-inflammatory properties of curcumin, a major constituent of Curcuma longa: a review of preclinical and clinical research. *Alternative Medicine Review* 14.
- Izui S, Sekine S, Maeda K, Kuboniwa M, Takada A, et al. (2016) Antibacterial activity of curcumin against periodontopathic bacteria. *Journal of Periodontology* 87: 83-90.
- Gogeneni H (2017) Porphyromonas gingivalis infection in gestational diabetes mellitus and survival in tobacco smokers. Doctor of Philosophy in Interdisciplinary Studies Electronic Theses and Dissertations, University of Louisville, Louisville, KY.
- Ranjbar Mohammadi M, Rabbani S, Bahrami SH, Joghataei M, Moayer F (2016) Antibacterial performance and in vivo diabetic wound healing of curcumin loaded gum tragacanth/poly (ϵ -caprolactone) electrospun nanofibers. *Materials Science and Engineering* 69: 1183-1191.
- Gupta T, Singh, J Kaur, S Sandhu, S Singh, et al. (2020) Enhancing bioavailability and stability of curcumin using solid lipid nanoparticles (CLEN): a covenant for its effectiveness. *Frontiers in Bioengineering Biotechnology* 8: 879.
- Sandhu SK, Kumar S, Raut J, Singh M, Kaur S, et al. (2021) Systematic Development and Characterization of Novel, High Drug-Loaded, Photostable, Curcumin Solid Lipid Nanoparticle Hydrogel for Wound Healing. *Antioxidants* 10.
- Schmolka IR (1972) Artificial skin I Preparation and properties of pluronic F-127 gels for treatment of burns. *Journal of Biomedical Materials Research* 6: 571-582.
- Maheshwari M, Miglani G, Mali A, Paradkar A, Yamamura S (2006) Development of tetracycline-serratiopeptidase-containing periodontal gel: formulation and preliminary clinical study. *AAPS Pharm Sci Tech* 7.
- Gupta C, Juyal V, Nagaich U (2018) Formulation and Optimization of Thermosensitive In-Situ Gel of Moxifloxacin Hydrochloride for Ocular Drug Delivery. *International Journal of Applied Pharmaceutics* 10: 123-130.
- Vadnere M, Amidon G, Lindenbaum, S, L Haslam, J (1984) Thermodynamic studies on the gel-sol transition of some pluronic polyols. *International Journal of Pharmaceutics* 22: 207-218.

15. Brand Williams W, Cuvelier ME, Berset C (1995) Use of a free radical method to evaluate antioxidant activity. *Food Science Technology* 28: 25-30.
16. Espin JC, Soler Rivas C, Wichers HJ (2000) Characterization of the total free radical scavenger capacity of vegetable oils and oil fractions using 2, 2-diphenyl-1-picrylhydrazyl radical. *Journal of Agricultural Food chemistry* 48: 648-656.
17. Garala K, Joshi P, Shah M, Ramkishan A, Patel J (2013) Formulation and evaluation of periodontal in situ gel. *International Journal of Pharmaceutical Investigation* 3: 29.
18. Nasra MM, Khiri HM, Hazzah HA, Abdallah OY (2017) Formulation, in-vitro characterization, and clinical evaluation of curcumin in-situ gel for treatment of periodontitis. *Drug Delivery* 24: 133-142.
19. Costa P, Lobo, JMS (2001) Modeling and comparison of dissolution profiles. *European Journal of Pharmaceutical Sciences* 13: 123-133.
20. Oral health 2020; web page: <https://www.who.int/news-room/fact-sheets/detail/oral-health> accessed on 01-07-2021'



This work is licensed under Creative Commons Attribution 4.0 License
DOI: [10.19080/CTBEB.2021.20.556032](https://doi.org/10.19080/CTBEB.2021.20.556032)

**Your next submission with Juniper Publishers
will reach you the below assets**

- Quality Editorial service
- Swift Peer Review
- Reprints availability
- E-prints Service
- Manuscript Podcast for convenient understanding
- Global attainment for your research
- Manuscript accessibility in different formats
(Pdf, E-pub, Full Text, Audio)
- Unceasing customer service

Track the below URL for one-step submission
<https://juniperpublishers.com/online-submission.php>